

Poly(vinyl alcohol) Blend Film with *m*-Aramid as an *N*-halamine Precursor for Antimicrobial Activity

Jaewoong Lee,¹ Hyun Suk Whang²

¹Kolon Industries, Inc., Gumi 730-030, South Korea

²Fiber and Polymer Science Program, North Carolina State University, Raleigh, North Carolina 27695

Received 27 October 2009; accepted 28 December 2010

DOI 10.1002/app.34055

Published online 17 June 2011 in Wiley Online Library (wileyonlinelibrary.com).

ABSTRACT: Poly(vinyl alcohol) (PVA) was blended with *m*-aramid as an *N*-halamine precursor for imparting antimicrobial activity. A series of PVA/*m*-aramid blend films were produced with different ratios of PVA/*m*-aramid by weight (100/0, 100/2, 100/6, 100/10, and 100/50). The films were characterized using Fourier transform infrared spectroscopy (FTIR), differential scanning calorimetry (DSC), wide-angle X-ray diffraction (WAXD), and thermogravimetric analysis (TGA). The FTIR spectra of the PVA/*m*-aramid blends are a combination of the spectra of pure PVA and of pure *m*-aramid. However, the peak intensity in the *m*-aramid decreases with decreasing *m*-aramid content from 50 to 2 wt % in PVA. It implies the compatibility of *m*-aramid in the PVA/*m*-aramid blend films. Furthermore, a single glass transition temperature (T_g) for all blend films by DSC confirms that

PVA/*m*-aramid is successfully miscible. The crystallinity of PVA/*m*-aramid blend films decreases slightly with increasing *m*-aramid content in the blend films. This agrees with the results obtained by WAXD. However, melting point and thermal stability of the blend films increases with increasing *m*-aramid content in the blend films. Chlorinated PVA/2% *m*-aramid blend film produces about 5.7 log reduction of both Gram-positive and Gram-negative bacteria at 30 min contact, implying sufficient antimicrobial activity. Therefore, PVA/*m*-aramid blend films may serve as a novel material for biomedical applications. © 2011 Wiley Periodicals, Inc. *J Appl Polym Sci* 122: 2345–2350, 2011

Key words: PVA; *m*-aramid; *N*-halamine; antimicrobial activity; film

INTRODUCTION

Poly(vinyl alcohol) (PVA) is one of the synthetic, biodegradable, biocompatible, water-soluble polymers used in many applications, such as textile sizing agent, emulsifier, food packaging, and lining of feminine hygiene products. It is produced industrially by the polymerization of vinyl acetate to poly(vinyl acetate) (PVAc), followed by hydrolysis of PVAc to PVA. Depending on the degree of hydrolysis, a variety of PVA may be produced ranging from partially to fully hydrolyzed grades. Blending is an important process for developing industrial applications of polymeric materials. There has been a considerable amount of research toward creating PVA blend materials with desirable characteristics and properties by adding other polymers. More recently, PVA blends could be cast as films and applied as biomedical materials, such as wound dressings, dialysis membranes, and drug delivery substances.^{1–5}

There has been a growing interest in the applications of *N*-halamine antimicrobials to polymers and fibers.^{6–10} *N*-halamines refer to compounds that con-

tain one or more nitrogen–halogen covalent bonds. It is reported that *N*-halamine structures containing adjacent α -hydrogens of a nitrogen–halogen bond are less effective in the preparation of stable *N*-halamine. This may be due to the fact that the adjacent α -hydrogen of a nitrogen–halogen bond causes dehydrohalogenation. *N*-halamine compounds containing nitrogen with no adjacent α -hydrogen are preferred as *N*-halamine precursors.^{6,7} Poly(*m*-phenyleneisophthalamide), *m*-aramid known as Nomex in the industry, is a high-performance aromatic polyamide, which has a wide variety of applications in daily life. Furthermore, it has been proposed as an *N*-halamine precursor because no adjacent α -hydrogen of a nitrogen–halogen bond makes extremely difficult the elimination of halogen after chlorination.^{6,11} The combination of *m*-aramid and polymeric materials, such as cellulose and polyethylene terephthalate (PET), has already been reported to have antimicrobial properties.^{6,12} However, little research has been done on the blend of PVA and *m*-aramid. The PVA/*m*-aramid blend will have great potential for a variety of biomedical applications as an antimicrobial plastic backing sheet in such products as packaging, linings of feminine sanitary napkins, and adult incontinence products. It will also be able to be used as a coating for sports textiles.

Correspondence to: H. S. Whang (hswhang@ncsu.edu).

In this study, PVA/*m*-aramid blend films were prepared with various compositions. The blend films were characterized using Fourier transform infrared spectroscopy (FTIR), differential scanning calorimetry (DSC), wide-angle X-ray diffraction (WAXD), and thermogravimetric analysis (TGA). In addition, the antimicrobial efficacy of the PVA/*m*-aramid blend films was investigated.

EXPERIMENTAL

Materials

PVA, more than 99.9% hydrolyzed granule, was obtained from Kolon Industries (Korea). The degree of polymerization ranged from 4000 to 4300. The *m*-aramid was a DuPont fiber product. The ionic liquid, 1-butyl-3-methylimidazolium chloride, was purchased from Aldrich Chemical Company (Milwaukee, WI) and was used as received. Bacterial cultures of *Staphylococcus aureus* (ATCC 6538) and *Escherichia coli* O157:H7 (ATCC 43895) used were from the American Type Culture Collection (Rockville, MD), and Trypticase soy agar was from Difco Laboratories (Detroit, MI).

Preparation of PVA/*m*-aramid blend film

The *m*-aramid fiber was washed with water, ethanol, and acetone to remove impurities and was then air-dried. A weight of 1.5 g of *m*-aramid was stirred into 100 g of 1-butyl-3-methylimidazolium chloride for 24 h at 85°C. A weight of 15 g of PVA was added into the solution to produce a 10% solution of *m*-aramid in the PVA blend. This mixture was also stirred for 24 h at 85°C. Five different solutions were made with the following ratios of PVA/*m*-aramid by weight: 100/0, 100/2, 100/6, 100/10, and 100/50. A film maker (Baker Applicator, Yoshimitsu, Japan) was used to produce PVA/*m*-aramid blend film. The PVA/*m*-aramid solutions were coagulated on film-making plates in a methanol bath at -20°C for 30 min and were subsequently washed with distilled water for two times. The films were dried at ambient temperature for 48 h before characterization. The thickness of all the films was about 300 μm on average ($n = 5$).

Characterization of PVA/*m*-aramid blend film

Fourier transform infrared spectroscopy

Spectrum GX FTIR Spectrometer (Bruker Co., Germany) was used for observing the infrared spectra of samples between 650 and 4000 cm^{-1} with a resolution of 2 cm^{-1} . The PVA/*m*-aramid blend films were observed by attenuated total reflectance.

Differential scanning calorimetry

DSC experiments of the films were performed with a DSC 2920 (TA Instruments, New Castle, DE, USA) under nitrogen purge gas and at a heating rate of 20°C/min. Before collecting the DSC data, the samples were heated to 280°C and then cooled down to room temperature at a rate of 100°C/min.

Wide-angle X-ray diffraction

X-ray diffraction data were collected from film samples under the following conditions: MiniFlex (Rigaku) X-ray diffractometer, Cu Ka radiation with the voltage at 30 kV, the current at 15 mA, and scanning speed at $2\theta = 5^\circ/\text{min}$ over the range $2\theta = 10\text{--}40^\circ$.

Thermogravimetric analysis

Thermogravimetric analyzer (TGA) scans were obtained with a TGA 2950 (TA Instruments, New Castle, DE, USA). Film samples were placed in an open platinum pan that was hung in the furnace. The weight percentage of remaining materials in the pan was recorded during heating from 30 to 600°C at a heating rate of 20°C/min. Nitrogen was used as the purge gas.

Chlorination and titration

A commercial 4.5% sodium hypochlorite solution was diluted to 3300 ppm of the commercial strength with distilled water. The diluted solution was applied to chlorinate the PVA/*m*-aramid blend films, and the PVA/*m*-aramid blend films were soaked in the solution (pH buffered to 7 with acetic acid) at ambient temperature for 60 min and rinsed with an excess of distilled water. Then, the samples were dried at 45°C for 2 h to remove any unbounded chlorine. An iodometric/thiosulfate titration procedure was employed to analyze the oxidative chlorine content. A volume of 100-mL distilled water was prepared with 1 mL of acetic acid followed by adding 0.1 g of KI. After the treated PVA/*m*-aramid blend films were soaked in the solution for over 12 h, sodium thiosulfate solution was added to titrate the amount of starch which stands for the amount of oxidative chlorine. The $[\text{Cl}^+]\%$ in the sample was calculated with the following equation:

$$[\text{Cl}^+]\% = (V \times N \times 35.45) / (W \times 2 \times 10)$$

where $[\text{Cl}^+]\%$ is the wt % of oxidative chlorine on the sample, V is equal to the volume of the titrant [sodium thiosulfate solution (mL)], N is equal to the normality of the titrant, and W is the weight of the sample (g). The constants 35.45, 2, and 10 are the molecular weight of Cl, the change in oxidation state

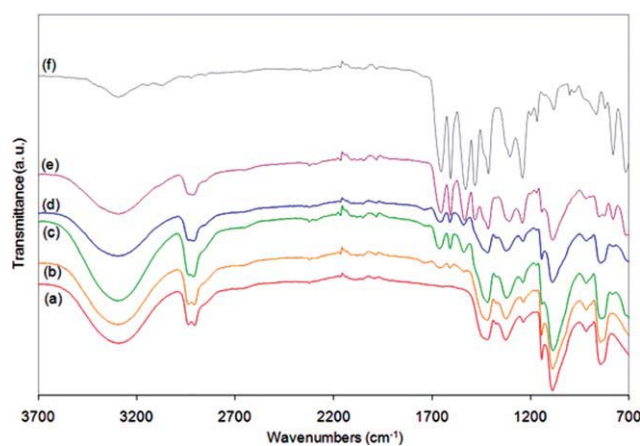


Figure 1 FTIR spectra of (a) PVA film, (b) *m*-aramid 2%, (c) *m*-aramid 6%, (d) *m*-aramid 10%, (e) *m*-aramid 50%, and (f) *m*-aramid film. [Color figure can be viewed in the online issue, which is available at wileyonlinelibrary.com.]

of Cl during titration, and a unit normalization factor to give % Cl, respectively.

Antimicrobial test

The control and chlorinated films were challenged with *Staphylococcus aureus* (ATCC 6538) and *Escherichia coli* O157:H7 (ATCC 43895) using a modified AATCC Test Method 100-1999. Bacterial suspensions (25 μ L) made with pH 7 phosphate buffer were added to one inch square sample swatches. A second swatch was sandwiched over the first to ensure contact between the suspension and the film. After contact times of 1, 5, and 30 min, the samples were quenched with 5.0 mL of sterile 0.02N sodium thio-sulfate solutions. The quenched samples were diluted using pH 7 phosphate buffer and plated on Typticase soy agar. The plates were incubated at 37°C for 24 h, and the number of bacteria was counted to determine the presence or absence of viable bacteria.

RESULTS AND DISCUSSION

Characterization of PVA/*m*-aramid blend film

The prepared PVA/*m*-aramid blend films were characterized using FTIR, DSC, WAXD, and TGA. Figure 1 shows the FTIR spectra of the pure PVA, pure *m*-aramid, and the different PVA/*m*-aramid blends. Similar to those found in the literature,^{13,14} the pure PVA exhibits a number of absorption peaks at about 3288, 2933, 1428, 1330, 1236, 1144, and 854 cm^{-1} , which were attributed to ν (O—H), ν (C—H), δ (CH—OH), δ (CH—OH), ω (CH), ν (C—O), and ν (C—C) vibrational modes, respectively. The pure *m*-aramid shows distinguished absorption features at about 3290, 1662, 1610, 1531, 1305, and 1238 cm^{-1} ,

which are assigned to the N—H stretching vibration, amide C=O stretching, C=C stretching vibrations of aromatic ring, N—H in-plane bending, and C—N stretching coupled modes of the C—N—H group, aromatic C—N stretching, and C—N stretching modes of *m*-aramid, respectively.

When the spectra of the PVA and the PVA/*m*-aramid blend films are compared, new bands appearing in the 1662, 1610, 1531, 1305, and 1238 cm^{-1} region are assigned to the amide C=O stretching, C=C stretching vibrations of aromatic ring, N—H in-plane bending and C—N stretching coupled modes of the C—N—H group, aromatic C—N stretching, and C—N stretching modes of *m*-aramid, respectively. In general, the spectra of the PVA/*m*-aramid blends are very similar to those of pure PVA and of pure *m*-aramid. However, the peak intensity in the PVA/*m*-aramid blends from that of the pure *m*-aramid decreases with decreasing *m*-aramid content from 50 to 2 wt % in PVA. This trend implies the presence of *m*-aramid in the PVA/*m*-aramid blend films.

According to the results in the literature,^{5,15–17} FTIR may be used to verify the miscibility of the PVA/*m*-aramid blend. If FTIR reveals the existence of intermolecular interactions between PVA and *m*-aramid in the blend, the absorption band at about 3288 cm^{-1} in the PVA film may be shifted to lower wavenumber with increasing of *m*-aramid content. This shift is due to the hydrogen bonding interaction between the O—H group of the PVA and the N—H group of the *m*-aramid. Such a shift indicating this interaction shows that *m*-aramid is compatible with PVA in the blend. In this study, the frequency shift of the 3288 cm^{-1} band in the PVA to a lower wavenumber did not significantly change when *m*-aramid content in the blend films increased. This may be due to the fact that the N—H stretching vibration in the *m*-aramid at about 3290 cm^{-1} is in a very similar region to the stretching vibration band of O—H in the PVA. However, we have found that *m*-aramid forms a clear homogeneous blend with PVA. Hence, it indicates the miscibility between the PVA and *m*-aramid in the blend.

One of the most commonly used methods to determine blend miscibility is to determine the glass transition temperature (T_g) of the blend. Hence, DSC technique was used to confirm the miscibility of the PVA and the *m*-aramid blend system. Figure 2 shows the DSC curves of the PVA, *m*-aramid, and PVA/*m*-aramid blend films. The results are summarized in Table I. Only one single T_g is observed for all blend films, indicating that the PVA/*m*-aramid is miscible. In addition, the T_g values increase with increasing *m*-aramid content in PVA/*m*-aramid blend films. This result also supports that the blend films have sufficient miscibility.

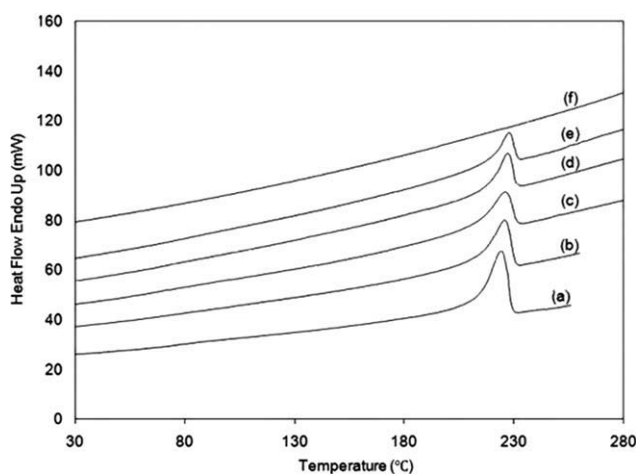


Figure 2 DSC curves of (a) PVA film, PVA blended with (b) *m*-aramid 2%, (c) *m*-aramid 6%, (d) *m*-aramid 10%, (e) *m*-aramid 50%, and (f) *m*-aramid film.

The degree of crystallinity of PVA/*m*-aramid blend films was calculated based on the following equation.

$$\chi_c = \frac{\Delta H_m}{w\Delta H_m^0}$$

where w is the weight fraction of PVA in the blend films, ΔH_m is the heat of fusion, and ΔH_m^0 is the heat of fusion of a purely crystalline form of PVA and has a value of 150 J/g.¹⁴ The crystallinity of PVA/*m*-aramid blend films decreases with increasing *m*-aramid content as shown in Table I. The decrease in crystallinity is possibly due to the interaction between PVA and *m*-aramid as well as to a substantial amorphous region in *m*-aramid. The diffraction curve of the pure *m*-aramid film exhibits a broad peak, which shows a substantial amorphous region and thus a low degree of crystalline orientation. In addition, the molecular conformation of *m*-aramid in the crystalline region is assumed to have high energy barrier to internal rotations of the phenylene-amide and C—N bonds, hence preventing the *m*-aramid molecule from transforming into a fully extended chain conformation. The decrease in crys-

TABLE I
The Glass Transition Temperature, Melting Temperature, Heat of Fusion, and Crystallinity of PVA/*m*-Aramid Blended Films

<i>m</i> -Aramid content (%)	Weight fraction of <i>m</i> -aramid	T_g (°C)	T_m (°C)	ΔH_m (J/g)	χ_c (%)
0	0	70.7	224.7	67.7	45.1
2	0.02	76.9	226.1	60.9	41.4
6	0.06	78.5	227.4	55.8	39.6
10	0.09	78.3	227.7	50.2	37.2
50	0.33	84.5	229.1	28.4	37.8

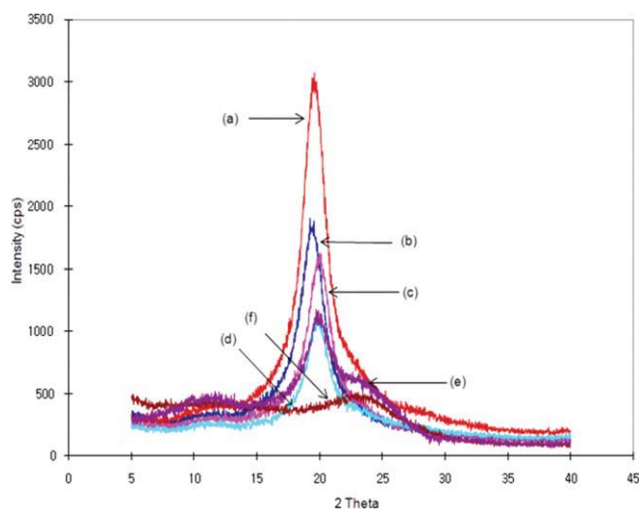


Figure 3 Wide-angle X-ray diffraction patterns of (a) PVA film, (b) *m*-aramid 2%, (c) *m*-aramid 6%, (d) *m*-aramid 10%, (e) *m*-aramid 50%, and (f) *m*-aramid film. [Color figure can be viewed in the online issue, which is available at wileyonlinelibrary.com.]

tallinity shown by DSC was further supported by WAXD as shown in Figure 3. The pure PVA exhibits one main peak at around $2\theta = 20^\circ$, corresponding to the (101) plane of the PVA semicrystalline structure.¹⁸ However, the peak intensity of the PVA/*m*-aramid blend films decreases from that of the pure PVA film. Furthermore, the crystallinity decreases steadily with an increasing of *m*-aramid content.

In terms of the melting temperatures of the PVA/*m*-aramid blend films, the temperature increases from 226 to 229°C as the *m*-aramid contents increase from 2 to 50%, indicating the presence of interaction between PVA and *m*-aramid. It is well known that *m*-aramid has been used for thermal protective applications because of its outstanding heat resistance.¹⁹ Hence, the higher melting temperature of the PVA/*m*-aramid blend films is indicative of the excellent heat resistance of *m*-aramid. Thermogravimetric measurement was carried out for the PVA, PVA/*m*-aramid blend, and *m*-aramid films. Figure 4 shows the thermal stability and decomposition behavior of the films. In general, the thermal decomposition of PVA/*m*-aramid blend films shifts toward a higher temperature range than that of the PVA film, which confirmed the enhancement of thermal stability of the blend films by the addition of *m*-aramid.

Chlorination and titration

The oxidative chlorine content of the PVA/*m*-aramid blend films at *m*-aramid content from 2 to 50 wt % is shown in Figure 5. The results in Figure 5 demonstrated that 2, 6, 10, and 50 wt % of *m*-aramid in the blend films provided 0.26, 0.73, 1.49, and 3.90 [Cl⁺]% after chlorination. In general, increasing the

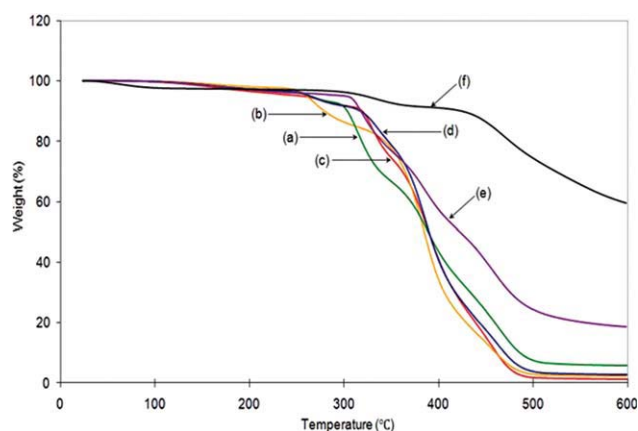


Figure 4 TGA curves of (a) PVA film, (b) *m*-aramid 2%, (c) *m*-aramid 6%, (d) *m*-aramid 10%, (e) *m*-aramid 50%, and (f) *m*-aramid film. [Color figure can be viewed in the online issue, which is available at wileyonlinelibrary.com.]

concentration of *m*-aramid in the blend films caused increase in the oxidative chlorine content in the films. This may be due to the fact that a higher concentration of *m*-aramid in the blended films has a higher content of N–H bonds, indicating more capability of generating chlorine charge in the blend films. In addition, increasing the concentration of *m*-aramid in the blend films caused a decrease in crystallinity. This allows greater water penetration into the film. Thus, increasing the concentration of *m*-aramid in the blend films may increase the oxidative chlorine.

Antimicrobial efficacy

The unchlorinated and chlorinated PVA/*m*-aramid blend films were challenged with *S. aureus* (Gram-positive) and *E. coli* O157:H7 (Gram-negative). The antimicrobial test results of the PVA/2% *m*-aramid blend films are shown in Table II. The unchlorinated samples show that a small degree of log reduction

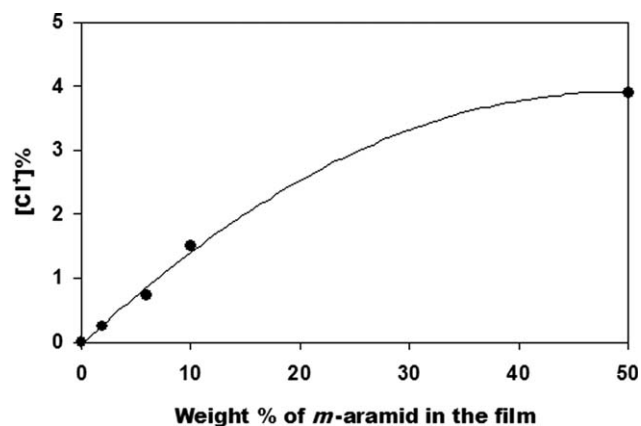


Figure 5 The oxidative chlorine content of the PVA/*m*-aramid blend films at various concentrations of *m*-aramid.

against *S. aureus* and *E. coli* O157:H7 occurred at 30 min contact time; the blend films show about 0.26 and 1.34 log reductions against *S. aureus* and *E. coli* O157:H7, respectively. The reduction of unchlorinated samples, however, was due to adhesion of bacteria to the samples instead of to inactivation. After chlorination, the blend films produce about 5.7 log reduction against both *S. aureus* and *E. coli* O157:H7 at 30 min contact time. It indicates that antimicrobial properties in the PVA/2% *m*-aramid blend films are sufficiently active against a broad spectrum of bacteria. It should also be noted that the antimicrobial activity may not be enhanced with increasing *m*-aramid content in the blend films up to 50 wt % in PVA. A significant increase in chlorine content can sufficiently enhance the hydrophobicity of the surface with increasing *m*-aramid content in the blend films. Hence, the antimicrobial activity will be decreased with increasing *m*-aramid content in the blend films.²⁰ Therefore, the PVA/2% *m*-aramid blend films may provide better antimicrobial activity than blends with higher concentration of *m*-aramid.

TABLE II
Antimicrobial Efficacy Against Microorganisms

Samples ^a	Contact time (min)	<i>Staphylococcus aureus</i> ^b			<i>E. coli</i> O157:H7 ^c		
		Bacterial no. (cfu/mL)	Total bacteria (cfu/sample)	Log reduction	Bacterial no. (cfu/mL)	Total bacteria (cfu/sample)	Log reduction
Control	1	8.23×10^4	3.54×10^5	0.19	5.87×10^4	2.99×10^5	0.28
	5	7.90×10^4	3.20×10^5	0.23	7.32×10^3	3.55×10^4	1.21
	30	7.05×10^4	3.01×10^5	0.26	6.21×10^3	2.61×10^4	1.34
Chlorinated ^d	1	2.98×10^2	2.06×10^3	2.42	6.47×10^2	5.11×10^3	2.05
	5	5.47×10^1	1.10×10^2	3.70	7.43×10^1	8.75×10^2	2.82
	30	0	0	5.74	0	0	5.76

^a 2 wt % of *m*-aramid in PVA.

^b Total bacteria: 5.45×10^5 cfu/sample.

^c Total bacteria: 5.71×10^5 cfu/sample.

^d $[Cl^+]%$ = 0.26.

CONCLUSIONS

PVA was blended with *m*-aramid as an *N*-halamine precursor for imparting antimicrobial activity. After blending *m*-aramid in PVA, new bands appearing in the 1662, 1610, 1531, 1305, and 1238 cm^{-1} region are assigned to the amide C=O stretching, C=C stretching vibrations of aromatic ring, N—H in-plane bending and C—N stretching coupled modes of the C—N—H group, aromatic C—N stretching, and C—N stretching modes of *m*-aramid, respectively. However, the peak intensity in the *m*-aramid decreases with decreasing of *m*-aramid contents from 50 to 2 wt % in PVA. Therefore, it implies the presence of *m*-aramid in the PVA/*m*-aramid blend films. DSC confirmed the miscibility of the PVA and *m*-aramid blend film. A single T_g for all blend films confirms a successful miscibility. The crystallinity of PVA/*m*-aramid blend films decreases somewhat with increasing *m*-aramid content. This is due to the interaction between PVA and *m*-aramid as well as to a substantial amorphous region in *m*-aramid. The decrease in crystallinity from DSC was further supported by WAXD. However, melting point and thermal stability of the blend films increases with increasing *m*-aramid content in the blend films. In terms of antimicrobial activity, chlorinated PVA/2% *m*-aramid blend film produces about 5.7 log reduction against both *S. aureus* and *E. coli* O157:H7 at 30 min contact, indicating sufficient antimicrobial activity. These results show a great potential for a variety of biomedical applications.

References

1. Wang, L. C.; Chen, X. G.; Zhong, D. Y.; Xu, Q. C. *J Mater Sci: Mater Med* 2007, 18, 1125.
2. Galya, T.; Sedlarik, V.; Kuritka, I.; Novotny, R.; Sedlarikova, J.; Saha, P. *J Appl Polym Sci* 2008, 100, 3178.
3. Sun, C.; Qu, R.; Ji, C.; Meng, Y.; Wang, C.; Sun, Y.; Qi, L. *J Nanopart Res* 2009, 11, 1005.
4. Wang, Q.; Du, Y.; Fan, L. *J Appl Polym Sci* 2005, 96, 808.
5. Aoi, K.; Nakamura, R.; Okada, M. *Macromol Chem Phys* 2000, 201, 1059.
6. Lee, J.; Broughton, R. M.; Worley, S. D.; Huang, T. S. *J Eng Fibers Fabr* 2007, 2, 25.
7. Kenawy, E.; Worley, S. D.; Broughton, R. M. *Biomacromolecules* 2007, 8, 1359.
8. Qian, L.; Sun, G. *J Appl Polym Sci* 2003, 89, 2418.
9. Lin, J.; Winkelmann, C.; Worley, S. D.; Kim, J.; Wei, C.; Cho, U.; Broughton, R. M.; Santiago, J. I.; Williams, J. F. *J Appl Polym Sci* 2002, 85, 177.
10. Ren, X.; Kocer, H. B.; Kou, L.; Worley, S. D.; Broughton, R. M.; Tzou, Y. M.; Huang, T. S. *J Appl Polym Sci* 2008, 109, 2756.
11. Sun, Y.; Sun, G. *Ind Eng Chem Res* 2004, 43, 5015.
12. Kim, S. S.; Kim, J.; Huang, T. S.; Whang, H. S.; Lee, J. *J Appl Polym Sci* 2009, 114, 3840.
13. Villar-Rodi, S.; Paredes, J. I.; Martinez-Alonso, A.; Tascon, J. M. D. *Chem Mater* 2001, 13, 4297.
14. Finch, C. *Polyvinyl Alcohol Properties and Application*; John Wiley & Sons: New York, 1973.
15. Jia, Y. T.; Gong, J.; Gu, X. H.; Kim, H. Y.; Dong, J.; Shen, X. Y. *Carbohydr Polymer* 2007, 67, 403.
16. Cui, L.; Yeh, J.; Wang, K.; Fu, Q. *J Polymer Sci Part B: Polymer Phys* 2008, 46, 1360.
17. Yi, J.; Goh, S. H. *Polymer* 2005, 46, 9170.
18. Koji, N.; Tomonori, Y.; Kenji, I.; Fumio, S. *J Appl Polym Sci* 1999, 74, 133.
19. Jain, A.; Vijayan, K. *Bull Mater Sci* 2002, 25, 341.
20. Ren, X.; Akdag, A.; Kocer, H. B.; Worley, S. D.; Broughton, R. M.; Huang, T. S. *Carbohydr Polymer* 2009, 78, 220.